CHAPTER 4

Enhancement of nonlinear optical properties of indole based dyes through electron acceptor and π-linker for dye-sensitized solar cell applications

Abstract

Six indole based thiazole substituted donor-π-acceptor molecules are designed and their nonlinear optical properties (NLO) are evaluated theoretically. Different electron withdrawing groups and π-linkers are used to understand their role in tuning the NLO properties. The NLO properties of the molecules are analyzed in gas phase and in different solvent medium through the dipole moment, static polarizability, first and second hyperpolarizabilities. Efficiency of the molecules are studied through HOMO-LUMO gap, frontier molecular orbitals, light harvesting efficiency, ionization potential, electron affinity and reorganization energy for hole and electron. All the dyes show maximum absorption wavelength in the visible region. The computed absorption spectra are well correlated with the HOMO-LUMO gaps of the molecules. The HOMO-LUMO gaps of all the dyes are found to be small, which lead to large NLO response. Results indicate that hyperpolarizability increases with increasing strength of the electron withdrawing group. In addition to the study of nonlinear optical property, we also calculate relevant parameters related to photovoltaic cells for two designed dyes which emerge suitable for this purpose. Photovoltaic parameters such as electron injection efficiency, exciton binding energy, and open circuit photovoltage are evaluated for dye sensitized solar cells (DSSC) applications. This study shows that alkyne π-linkers are better than the alkene π-linkers for desired applications. Overall, this study highlights the optical and photovoltaic nature of the dyes and reveals the influence of different π-linkers and electron acceptors in designing new materials for NLO and DSSC applications.

4.1. Introduction

Organic compounds exhibiting strong nonlinear optical (NLO) response have become focus of applied research during recent years due to their potential applications in the field of optical storage, optical telecommunications, [1-4] high density optical materials,[5-7] integrated laser medicine,[8] fluorescence imaging[9] etc. Compared with inorganic materials, NLO materials based on organic skeleton are highly preferred,[10] because of their possible advantages such as lower cost, ease of processing, high electro-optic coefficients and so on.[11, 12] Chromophores with large hyperpolarizability together with the enhancement of other properties like high yield, robust thermal stability and excellent chemical as well as photo stability are of utmost importance in the development of efficient NLO materials.[13, 14] Such an organic NLO material is usually composed of push-pull chromophores. These types of chromophores contain π-conjugated bridge which is end-capped by donor (D) and acceptor (A) groups. The role of π-conjugated bridge is to provide a route for the ultrafast rearrangement of electric charges under an external electric field.[15] It is well known that large hyperpolarizability can be achieved by modifying the strength of donor and acceptor groups and also with the change in the nature and length of π-conjugated bridge.[16],[17] It is reported that with increasing strength of the electron withdrawing group (EWG)[18] and introduction of an additional electron-rich hetero atom into the donor moiety could effectively enhance the nonlinear optical properties.[19] The NLO chromophores crafted with thiophene,[20] locked phenyltetraene,[13] azo[21] and phenyltetraene-based[22] bridges are well known. It has been shown that five membered heteroatomic rings such as thiophene, pyrrole are superior as bridging groups compared to the aryl analogues,[23-25] as they significantly increase the electron density of the π-conjugated bridge. Logically, connection of a strong donor to an electron rich heterocycle and a strong electron acceptor to an electron deficient heterocycle will improve NLO response.[26] This influences us to design the investigated molecules in the present study where we choose thiazole unit as auxiliary π-conjugator. It is well known that the presence of thiazole unit in organic system enhances the coplanarity of the structure and its imine (–C=N–) group increases the electron accepting tendency.[27, 28] Previous studies have shown that when thiazole is substituted at the acceptor end, hyperpolarizability increases in comparison to oxazole and imidazole.[25, 29, 30]

Due to the excitation of photoelectron in a D-π-A system, an extensive charge transfer occurs and electron affluent donor unit experiences an intramolecular charge transfer to the electron deficient acceptor unit. The charge transfer phenomena in D-π-A system on semiconductor surface facilitates the electron injection properties of the sensitized dye.[31] This type of extensive charge transfer (CT) in such push-pull systems enhanced by the conjugation of π-bridge and the degree of non-centrosymmetric charge distribution leads to large NLO properties which has direct impact on the DSSC efficiency.[32] Some studies have revealed that thiazole based π-conjugated chromophores can be fabricated for small molecular organic solar cell which shows good power conversion efficiency.[33,34] So, inclusion of the thiazole unit into the molecule can improve the solar cell performance. Therefore, in addition to the study of nonlinear optical property, we also calculate some parameters related to photovoltaic cell for dye sensitized solar cells (DSSC) applications.

In the present work we choose indole as an electron donating group in the D-π-A system because of its good electronic and photonic properties.[35] There are several reports that reveal indole based chromophores possess high NLO [36-38] and photovoltaic properties. [39-42] Carboxylic acid is used in the anchoring part for DSSC application because of its stability and easy synthesis.[43] As hydrogen atom of indole is active, we also calculated NLO property of N-methyl indole as donor which can be synthesized easily[44, 45] and this is compared with the indole donor systems. In this investigation, thiazole ring with alkene or alkyne groups is used as π-linker whereas cyanide or carboxyl group attached with acrylonitrile is used as electron acceptor (Scheme 4.1). There are only a few reports in the literature where alkyne group have been used as π-conjugated linker which demonstrates high nonlinear response as well as high efficiency in organic DSSC.[46, 47] In this work, optoelectronic properties of the six newly designed molecules are investigated using density functional theory based method. The NLO properties of the molecules are analyzed in gas phase and in different solvent medium through the dipole moment, static polarizability, first and second hyperpolarizabilities. In addition to this, photovoltaic parameters for DSSC application such as electron injection efficiency, exciton binding energy and different chemical parameters such as softness, hardness, and chemical potential have been explored. Efficiency of the molecules are

studied through frontier molecular orbitals (FMO), absorption spectra, light harvesting efficiency (LHE), ionization potential (IP), electron affinity (EA) and reorganization energy. This work also reports, systematic study of the effect of solvent polarity on (hyper) polarizability. The object of the work is to reveal the photophysical and photovoltaic nature of the dyes and understand the influence of different π-linkers and electron acceptors.

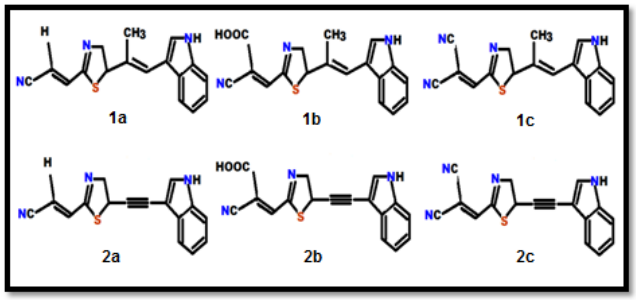

Scheme 4.1. Chemical structures of the indole-based dyes.

4.2. Theoretical Background

4.2.1. Nonlinear optical properties (NLO)

A good nonlinear optical (NLO) material has high polarizability and hyperpolarizability values. We have calculated static dipole moment (μ), mean polarizability (α), first-order hyperpolarizability (β) and second-order hyperpolarizability (γ) at the ground state geometry of the designed molecules. Dipole moment and mean polarizability was calculated using the following equations:[48]

$$\mu_{tot} = \sqrt{\mu_x^2 + \mu_y^2 + \mu_z^2} \qquad (4.1)$$

$$\alpha = \frac{1}{3}\left(\alpha_{xx} + \alpha_{yy} + \alpha_{zz}\right) \qquad (4.2)$$

α_{xx} , α_{yy}, α_{zz} are the polarizability tensor components.

The total first-order hyperpolarizability,[48] β_{total} can be expressed as:

$$\boldsymbol{\beta_{total}} = [(\boldsymbol{\beta_{xxx}} + \boldsymbol{\beta_{xyy}} + \boldsymbol{\beta_{zxx}})^2 + (\boldsymbol{\beta_{yyy}} + \boldsymbol{\beta_{yzz}} + \boldsymbol{\beta_{yxx}})^2 + (\boldsymbol{\beta_{zzz}} + \boldsymbol{\beta_{zxx}} + \boldsymbol{\beta_{zyy}})^2]^{1/2} \quad (4.3)$$

β_{xxx}, β_{xyy}, β_{zxx}, β_{yyy}, β_{yzz}, β_{yxx}, β_{zzz}, β_{zxx} and β_{yyy} are hyperpolarizability tensors along x, y and z direction.

The second-order hyperpolarizability, γ_{total}[49] is calculated using equation 4.4.

$$\boldsymbol{\gamma_{total}} = \frac{1}{5}[(\boldsymbol{\gamma_{xxxx}} + \boldsymbol{\gamma_{yyyy}} + \boldsymbol{\gamma_{zzzz}}) + 2(\boldsymbol{\gamma_{xxyy}} + \boldsymbol{\gamma_{yyzz}} + \boldsymbol{\gamma_{zzxx}}) \quad (4.4)$$

Ionization Potential (IP) and electron affinity (EA) signifies the energy changes of removing electron or adding holes and adding electron or removing hole from / to the neutral molecule. This can be expressed as:[50]

$$\boldsymbol{IP} = \boldsymbol{E_{Cation}} - \boldsymbol{E_{Neutral}} \text{ and } \boldsymbol{EA} = \boldsymbol{E_{Neutral}} - \boldsymbol{E_{Anion}} \quad (4.5)$$

E denotes energy of the respective molecules. Hole transport reorganization energy (λ_{hole}) and electron transport reorganization energy ($\lambda_{electron}$) are calculated as:[51]

$$\boldsymbol{\lambda_{hole}} = \boldsymbol{\lambda_1} + \boldsymbol{\lambda_2} = (\boldsymbol{E_0^*} - \boldsymbol{E_0}) + (\boldsymbol{E_+^*} - \boldsymbol{E_+})$$
$$\boldsymbol{\lambda_{electron}} = \boldsymbol{\lambda_3} + \boldsymbol{\lambda_4} = (\boldsymbol{E_0^*} - \boldsymbol{E_0}) + (\boldsymbol{E_-^*} - \boldsymbol{E_-}) \quad (4.6)$$

Here, E_0, E_+ and E_- represent the energy of neutral, cation and anion species in their optimized geometries. E_0^* and $E_{+/-}^*$ represent energy of neutral and cation / anion species with the geometries of the cation / anion and neutral species. .

4.2.2. Photovoltaic properties of dye sensitized Solar cell (DSSC)

The efficiency of electron injection process to the surface of conduction band of semiconductor and electron accumulation efficiency at the transparent conductive oxide electrode regulate the short-circuit current density (J_{sc}) of DSSC. The efficiency (η) of DSSC can be expressed using the following equation:[52]

$$\eta = \frac{\boldsymbol{J_{SC}}\ \mathbf{FF}\ \boldsymbol{V_{OC}}}{\mathbf{P_{IN}}} \quad (4.7)$$

where V_{OC} is the open-circuit photovoltage, which is the potential difference between the Fermi level of the electrons in the semiconductor and redox potential of the electrolyte. FF is the fill factor and P_{IN} is the input power of incident solar light. The short-circuit density (J_{SC}) in DSSC is determined as:[53]

$$J_{SC} = \int_{\lambda} \mathbf{LHE}(\boldsymbol{\lambda})\, \boldsymbol{\phi}_{\mathbf{inject}}\, \eta_{\mathbf{collect}}\, d\lambda \qquad (4.8)$$

LHE (λ) is light harvesting efficiency, ϕ_{inject} is the electron injection efficiency and $\eta_{collect}$ is the charge collection efficiency. Equation 4.8 describe that, large LHE and ϕ_{inject} of the sensitizer, assist to achieve high J_{SC} value. The LHE is described by:[54]

$$\boldsymbol{LHE = 1 - 10^{-A} = 1 - 10^{-f}} \qquad (4.9)$$

Where A (f) is the absorption (oscillator strength) of the dye. So, larger f value imparts higher light harvesting efficiency.

ϕ_{inject} is correlated with the free energy change (ΔG), which is linked to the electron injection process from the photoinduced excited state of the dye into the TiO_2 surface.[54, 55]

$$\boldsymbol{\phi}_{\mathbf{inject}} \propto \boldsymbol{f}\,(-\Delta \boldsymbol{G^{inject}}) \qquad (4.10)$$

$$\Delta \boldsymbol{G^{inject}} = \boldsymbol{E^{dye*} - E_{CB} = E^{dye} - E_{0\text{-}0} - E_{CB}} \qquad (4.11)$$

E^{dye*} and E^{dye} are the excited state and ground state oxidation potential energy of the dye. E_{CB} is reduction potential of TiO_2 conduction band. Herein we use, –4.0 eV for TiO_2. $E_{0\text{-}0}$ represents electronic vertical transition energy.[56] To achieve high energy-conversion efficiency, dye molecules should overcome the binding energy barrier, i.e., dye should hold low exciton binding energy (E_b). E_b is determined as:[57, 58]

$$\boldsymbol{E_b = E_g - E_x = E_{H-L} - \lambda_{max}} \qquad (4.12)$$

E_g is band gap of dye molecule and estimated as the difference of HOMO–LUMO energy and E_X is the optical band gap and defined as electronic vertical transition energy.

4.3. Computational Details

All the calculations are performed using Gaussian 09 programme package[59] at B3LYP/6-311++G(d,p)[60] level of theory otherwise stated elsewhere. The ground state geometry optimization of the designed molecules are carried out in gas phase and in different solvents such as toluene, dichloromethane (DCM), acetonitrile (MeCN), dimethylformamide (DMF) and dimethyl sulfoxide (DMSO). Optimization in the solvent phase has been done by applying the self-consistent reaction field (SCRF) incorporated in the polarizable continuum model (PCM).[61, 62] The vibrational frequency analysis of the

optimized structure is carried out at the same level of theory. No imaginary frequency was found which verify local minima of the optimized structures. To get vertical excitation energy at the ground state optimized geometry for the singlet-singlet excitation, time dependent density functional theory (TDDFT) calculations are performed. For the account of long range correction (LC) in TDDFT calculation the hybrid exchange-correlation functional CAM-B3LYP is used.[63] Multiwfn 3.3.6 program was used to analyze molecular orbital (MO) contributions from the groups of atoms.[64]

4.4. Results and Discussions

4.4.1. Geometrical structures

Here, Scheme 4.1 represents indole based molecules with different acceptor groups and π-linkers. The optimized geometries of the investigated molecules are given in Fig. S1 (Supporting information) and bond parameters are shown in Scheme S1 and Tables S1-S7 in the supporting information. Geometrical structure of a molecule is an important parameter in regulating its properties. The degree of delocalization influences the optical properties of the dye.[65] It is anticipated that an efficient dye should have coplanarity between the anchoring groups to the bridging unit and donor moiety which makes the electron transfer process smooth. With the introduction of alkyne π-linker in **2b** and **2c**, the planarity of the compound increases. For all the compounds the dihedral angle ϕ_1 which is formed between acceptor group and additional π- linker are nearly close to 180^o which indicates the planarity of the molecules. The dihedral angle ϕ_4 shown in Table S7 found between donor moieties and π-linkers are calculated to be 160.2^o, -163.7^o, -162.8^o, -10.8^o, -2.48^o and 179.8^o respectively. Compared to other molecules **2b** and **2c** show more planarity which suggests that introduction of the alkyne π-linker enhances planarity. Therefore, the calculated geometrical parameters impart that, planarity and delocalization of a molecule can be adjusted by varying the π-linkers and electron withdrawing groups which are of crucial importance in optoelectronic properties.

4.4.2. Frontier molecular orbitals

To gain more information about the molecular structure and electronic distribution of these molecules, frontier molecular orbital (FMO) analysis has been carried out. Molecular energy level diagram of the dyes are shown in 4.1. FMO theory is used to obtain information about the optical property of the organic molecules[66-68] and to predict the chemical stability of the dye.[69] Smaller energy gap (ΔE) between the highest occupied molecular orbital (HOMO) and lowest unoccupied molecular orbital (LUMO) influences the molecules to absorb light in the higher wave length region.[70] Also, HOMO-LUMO energy gap is an important parameter for prediction of chemical hardness and softness of a molecule.[71] High ΔE value reveals chemically hard molecules with high stability and low ΔE value indicates less stability, i.e., chemically soft molecule. Polarizability increases with the increase of the softness in a molecule which facilitates the NLO response.[72] Chromophores **1b**, **1c** and **2c** show lower HOMO-LUMO gap compared to the other compounds, which indicate that they should exhibit better NLO properties. We analyze the frontier molecular orbitals of the investigated dyes, represented in Fig. S8 (supporting information) where it is observed that, HOMOs for all the dyes are delocalized throughout the molecular framework and LUMOs are more concentrated in the acceptor and π-spacer region. Calculated energy values of HOMOs and LUMOs in different solvent phases are represented in Table S8 (supporting information) which demonstrates positive solvatochromism. From Fig. 4.1 it is seen that compound **1a**, **2a** and **2b** have approximately similar energy gaps, which suggest that π-conjugated linkers involved in this dyes have similar impact in the HOMO and LUMO energy levels. Although it has been found that substitution of alkene π-linkers (compound **1a**) by alkyne π-linker (compound **2a**) the HOMO-LUMO energy gap increases which is also reflected in the geometry of the molecules. The least band gap found for compound 1c (2.5 eV). The calculated HOMO-LUMO energy gaps of all the dyes are in the range of 2.5 eV to 2.99 eV. It may be noted that the competitive electron dragging nature of cyano group results π-electron delocalization throughout the molecular framework which is reflected in the energy level diagram (Fig. 4.1). With the variation of the strength of electron withdrawing groups, stabilization of LUMOs become more prominent than that

by the HOMOs. Overall, all the investigated dyes have smaller energy gaps. So, the studied dyes would exhibit excellent NLO properties.

To know more about the electronic property of the molecules, we calculate the composition of FMOs, which are presented in Fig. 4.2. Dye molecules have been segmented into 4 units- as acceptor, TH (thiazole), π-bridge and donor (indole). From the figure it can be found that donor unit stabilizes the HOMO whereas acceptor unit stabilizes the LUMO as the composition of the HOMO is dominated by the donor fragment. In all dye molecules, TH unit largely stabilizes the LUMO. It is interesting to note that in case of alkene substituted dyes, HOMO is more stabilized by π-bridge than thiazole ring whereas in case of alkyne substituted dyes reverse order is found. This may be due to more planarity achieved between the thiazole unit and π-bridge in case of alkyne substituted compounds which are in accordance with the geometrical parameters. The N atom of thiazole ring significantly enhances the π-conjugation of these molecules. This information helps us in designing molecule with suitable band gap for NLO and solar cell applications.

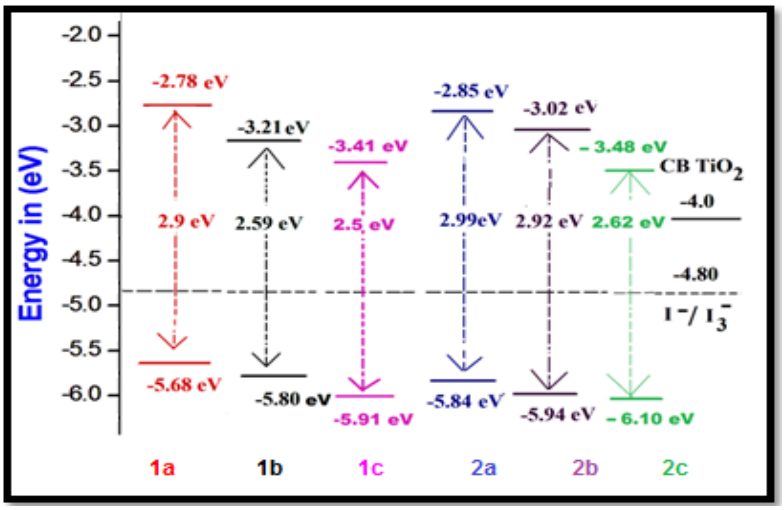

Fig. 4.1. Schematic energy level diagrams of the dyes in gas phase, the CB of TiO_2, and the electrolyte (I^-/I^-_3).

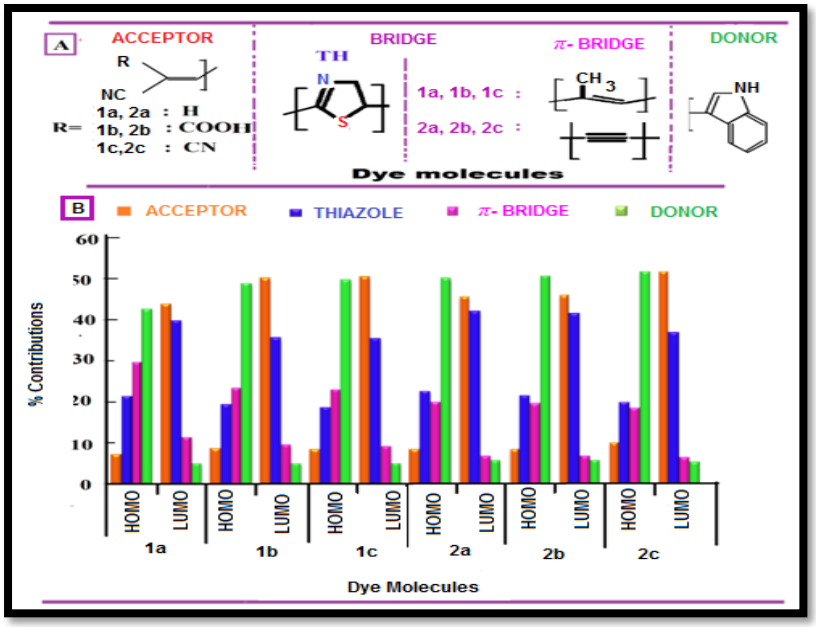

Fig. 4.2. Composition of frontier molecular orbitals (FMO) of various fragments of the indole based dyes (A) Different fragments involved in the calculation of percentage contribution to FMOs. (B) FMO composition (%).

4.4.3. Electron transfer process

For the desired photovoltaic performance, an appropriate energy band is necessary. Efficiency of the dye molecules in DSSC, hence, the electron injection process are determined by the electronic energy level of dye molecules which are related to the conduction band of the semiconductor surface. For this purpose, we take indole as electron donating group, cyanoacrylic acid as electron acceptor group and thiazole as additional π-conjugated linker. It is to be noted that for DSSC application, dye molecule must hold appropriate anchoring group to adsorb onto the semiconductor surface, therefore among the studied molecules, **1b** and **2b** where carboxylic acid groups are present are considered for further study in this direction. In DSSC, a sensitizer dye should hold several important properties like; (i) broad absorption spectrum, (ii) high molar extinction coefficient, (iii) strong anchoring group for the interaction with semiconductor electrode, (iv) appropriate redox potential to match electron injection, (v) HOMO of the dye must have low energy than the redox potential of the electrolyte and LUMO of the

dye must lie above the conduction band of semiconductor.[73-76] For thermodynamically spontaneous electron transfer process, LUMO of the dyes should be above the conduction band of TiO_2 (–4.0 eV) and HOMO of the dye should be below reduction potential of the electrolyte I^-/ I^-_3 (–4.8 eV). The HOMO and LUMO energy of compound **1b** and **2b** are –3.02 eV, –3.21 eV and –5.94 eV, –5.80 eV respectively (Fig. 4.1), which suggest that these dyes should give positive response. So, the dyes are capable to inject electron to the conduction band and easily restore electrons from the electrolyte in the photo-oxidation process. Fig. 4.1 exhibits the relative energy level of the investigated dye, along with conduction band of the TiO_2 and I^-/ I^-_3 as redox couple.

4.4.4. Absorption properties

Based on the optimized geometries of the compounds, the vertical excitation energy of the studied dyes in gas phase and in different solvent phases are calculated using CAM-B3LYP/6-311++G (d,p) level of theory. The vertical excitation energy, oscillator strength (*f*), maximum absorption wavelength (λ_{max}), light harvesting energy (LHE) were obtained for the lowest six singlet-singlet transition and are tabulated in Table 4.1 and Table S9 (supporting information), it has been found that when the π-bridge of compound **1a** is replaced with alkyne π-bridge in compound **2a** the absorption spectra of the dye molecules in gas phase are blue shifted by 15 nm. This is due to less planar structure and high HOMO-LUMO gap of **2a** compared to **1a** which is discussed earlier. The absorption maxima of the designed molecules are red shifted with increasing strength of EWG from a→ b → c for both alkene (by 42 nm and 10 nm) and alkyne π-linker series (by 10 nm and 36 nm). In polar solvent, expected red shift of the absorption wavelength is found for all the dyes. This may be ascribed to the lowering the energy of HOMO-LUMO gap (Table S8) in the polar environment. The highest absorption maxima found for compound 1c compare to other studied molecules. Among all the dyes **2a** has highest excitation energy (3.32 eV) and **1c** has lowest excitation energy (2.82 eV) in gas phase. All the dyes absorb light in the visible region of the spectrum. For all the cases, the absorption band is associated with HOMO → LUMO transition.

Light harvesting energy (LHE) is determined by the oscillator strength (*f*) of vertical excitation of the dye which is correlated with the intensity of the absorption spectra.[54] High oscillator strength gives high LHE which elevates the short circuit current density of the molecule. Calculated results of oscillator strength and light harvesting energy of the studied molecules are reported in the Table 4.1 and Table S9. Oscillator strength as well as LHE increases with the increase in bond character of the conjugated π-linker. Alkyne substituted π-linker exhibits highest value of oscillator strength and LHE among all the dyes. The order of LHE and *f is* as follows: **2c** > **2b** > **2a** > **1c** > **1b** > **1a**.

Table 4.1. Main electronic transitions, oscillator strength and light harvesting efficiency of indole-based dyes in gas phase at CAM-B3LYP/6-311++G(d,p) level of theory.

Dye	Excited energy (eV)	λ_{max} (nm)	*f*	Assignment	LHE
1a	3.19	389	0.9746	H – L 67.18%	0.894
1b	2.88	430	0.9961	H – L 67.37%	0.899
1c	2.82	440	1.0021	H – L 67.65%	0.901
2a	3.32	373	1.1300	H – L 66.63%	0.926
2b	3.24	383	1.1433	H – L 66.65%	0.928
2c	2.96	419	1.1570	H - L 67.12%	0.930

4.4.5. Dipole moment

Dipole moment (μ) of the organic molecule is one of the useful parameters which gives information about the charge distribution in the molecule, thereby assists to design molecule for optoelectronic applications. Dipole moment of the studied dyes are calculated at the B3LYP/6-311++G (d,p) level of theory in gas phase as well as in different polar solvents represented in Fig. S9 and Table S10 (supporting information). From Fig. S9, it can be found that strong EWG substituted π-acceptor (**1c** and **2c**) demonstrates maximum dipole moment of 13.09 Debye and 12.78 D in gas phase. As expected the dipole moment successively increases with increasing solvent polarity. In DMSO, the dipole moment of **1c** is 20.09 Debye.

4.4.6. Nonlinear optical properties

Hence, for the assessment of NLO properties of the investigated dyes, linear response, i.e., polarizability (α) and nonlinear response, i.e., hyperpolarizability (β and γ) need to be evaluated. To investigate the influence of π-conjugated linker and EWG at the π-acceptor position α, β and γ values are calculated and results are tabulated in Table 4.2. These are graphically represented in Fig. 4.3 and Fig. S10 (supporting information). The average polarizability ($\Delta\alpha$) (Fig. S10, panel A) of the investigated dyes are found in the following order: **2a** < **1a** < **1b** < **2b** < **2c** < **1c**. In most of the cases static polarizability is proportional to the dipole moment of the dyes.[77] It has been found that with increasing the strength of EWG at the π-acceptor region, push-pull effect increases hence $\Delta\alpha$ increases from a → b → c.

The second-order hyperpolarizability is connected with intramolecular charge transfer (ICT). Charge transfer occurs due to the flow of electron density from D to A moieties via π-bridge. When the external electric field interacts with the electron density of the molecule, dipole moments alter which influence NLO response.[78] It is reported that, 1st hyperpolarizability (β) depends on various factors such as, HOMO-LUMO gap, intra-molecular charge transfer, π-conjugation length, different substitution etc.[24, 79] Energy gap between HOMO and LUMO has a prominent effect on the hyperpolarizability of the molecule. For both alkene and alkyne substituted π-linker series with the decrease of HOMO-LUMO gap NLO response enhances. From Fig. 4.1 and Fig. S10 (panel B), it has been observed that, β values are inversely proportional to the HOMO-LUMO gap. Compound **2c** which has perfect planar geometry has highest β_{total} and γ_{total} values of 217× 10^{-30} esu and 540.2 ×10^{-36} esu. With the substitution of alkene π-linker by alkyne π-linker, β_{total} increases by 16.5× 10^{-30} esu in gas phase. The least value of 121×10^{-30} esu of β_{total} found for compound **1a**. From Table 4.2, we found the order of the β_{total} and γ_{total} is **1a** < **2a** < **2b** < **1b** < **1c** < **2c**. The higher hyperpolarizability values are responsible for electron delocalization of π-electrons. All the calculated results demonstrate that NLO property enhances with increasing power of EWG in electron acceptor region (a < b < c) and alkyne substituted π-linker is favoured over alkene substituted π-linker.

α, β and γ values show an increasing trend with the increase in solvent polarity presented in Fig. S10 and Table S10 (supporting information). β_{total} values of the studied dyes are in the range of 121 × 10^{-30} esu to 201 × 10^{-30} esu in gas phase which reaches in the range of 495 × 10^{-30} esu to 999 × 10^{-30} esu in DMSO. The increment of the polarizability and hyperpolarizability values can be assigned to the increase of dipole moment in the polar solvent. Polar solvent affects the environment of the NLO chromophores. Firstly, the electronic distributions of the incorporated dye molecules are changed compared to the gas phase, which is called static reaction field. Secondly, the external field is perturbed by the dielectric medium of solvent and local field is experienced by the chromophore.[80] From Table S10, it has been found that all the calculated $\Delta\alpha$, β and γ values are much higher. The maximum value of $\mu\beta$ obtained for compound **2c** of 2782×10^{-48} esu. $\mu\beta$ value ranges from 1208 ×10^{-48} esu to 2782 ×10^{-48} esu in gas phase and 6528×10^{-48} esu to 17, 104 ×10^{-48} esu in solvent phase. Computed β_{total} value of **1a**, **1b**, **1c**, **2a**, **2b** and **2c** dyes are 326, 522, 541, 370, 423 and 587 times greater than the value of urea. Therefore, the results indicate that among all the dyes **2c** is the most promising candidate for NLO application.

For comparison between indole and N-methyl indole (Scheme S1, supporting information) as donor in the push-pull systems, we have performed the NLO calculation at the B3LYP/6-311++G (d,p) level of theory in gas phase. The results indicate that methylation of indole ring enhances planarity of the system as the conjugation length increases. The energy difference between HOMO and LUMO of N-methyl indole is small compare to the indole based donor system which is shown in supporting information (Fig. S12). Computed $\Delta\alpha$, β and γ value of N-methyl indole dyes are tabulated in S11 and presented in Fig. S13 (supporting information). The maximum value of β_{total} of 257 × 10^{-30} esu and γ value of 614 × 10^{-30} esu found for N-methyl indole donor systems. So, it can be concluded that suitable substitution at indole moiety can improve the NLO property of the system and this also opens up possibilities for future studies.

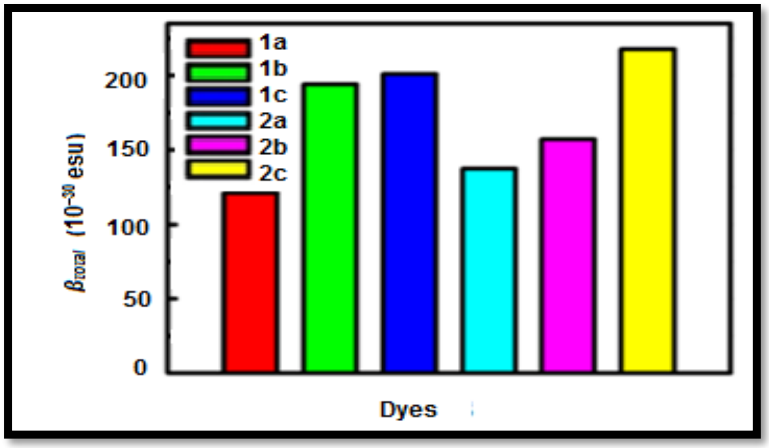

Fig. 4.3. First order hyperpolarizability of indole based dyes studied at the B3LYP/6-311++G (d,p) level of theory in gas phase.

Table 4.2. The dipole moment, static polarizability, first and second order hyperpolarizability of dyes studied at the B3LYP/6-311+G(d,p) level of theory in gas phase.

Molecule	μ Debye	$\Delta\alpha$ 10^{-24} esu	β_{total} 10^{-30} esu	γ 10^{-36} esu	$\mu\beta$ 10^{-48} esu
1a	9.99	46.95	121.00	399.45	1208.79
1b	9.24	52.73	193.94	501.70	1792.01
1c	13.09	53.27	200.84	501.78	2628.99
2a	9.93	46.01	137.49	433.31	1365.28
2b	10.92	49.63	157.13	470.82	1715.86
2c	12.78	52.21	217.70	540.2	2782.20

4.4.7. Photovoltaic properties

For the DSSC, dye molecule must hold appropriate anchoring group to adsorb onto the semiconductor surface, therefore among the studied molecules, **1b** and **2b** hold the criteria of photovoltaic process. An efficient dye should possess high photo-electric conversion efficiency, rapid electron injection efficiency from the excited state of the dye to the conduction band of the semiconductor and regeneration of the oxidized dye by the electrolyte. For fast electron transfer, low reorganization energy (ΔG_{reg}) is necessary. The

ΔG_{reg} can be calculated by the following eqation: $\Delta G_{reg} = E(I^-/I_3^-) - E_{dye}$. For the efficient electron injection process from the dye molecule to TiO2 surface ΔG^{inject} should be negative. Electron injection free enthalpy (ΔG^{inject}), E^{dye}, E^{dye*}, E_{0-0} and ΔG_{reg} are summarized in Table 4.3. Both the compounds show negative value of ΔG^{inject} and low reorganization energy. Therefore, the electron injection process is spontaneous and there is potential to get higher power conversion efficiency. Results indicate that, dye **2b** has higher electron injection efficiency than **1b**. The exciton binding energy of **1b** and **2b** molecules are very close (0.21 eV and 0.20 eV). The overall efficiency (η) of DSSC depends on the open circuit voltage (V_{OC}) as expressed in the equation no. 4.7. The values of short-circuit current density (*Jsc*), fill factor (FF), intensity of the incident solar light (P_{IN}) can be obtained from the current – voltage characteristics in the irradiated condition. V_{OC} can be expressed by the following expression $eV_{OC} = E_{LUMO} - E_{CB}$.[77] This expression indicates that, higher value of LUMO energy results higher value of V_{OC}. Generally organic dyes experience low value of open circuit voltage due to the electron / dye cation recombination.[31] In this study we find high open circuit voltage. The computed values of eV_{OC} are given in Table 4.3. Results indicate that, dye **2b** shows higher electron injection efficiency and open circuit voltage. So, we infer that among the studied dyes, **2b** will show best performance in DSSC applications.

Table 4.3. E^{dye*} and E^{dye} is excited state and ground state oxidation potentials, E_{0-0} represents electronic vertical transition energy, ΔG_{inject} is electron injection free enthalpy, E_b denotes excitation binding energy and eV_{OC} represents open circuit voltage of the studied dyes at the B3LYP/6-311++G(d,p) level of theory in gas phase.

Dye	E^{dye} (eV)	E_{0-0} (eV)	E^{dye*} (eV)	ΔG_{inject} (eV)	ΔG_{reg} (eV)	E_b (eV)	eV_{OC} (eV)
1b	5.80	2.39	3.41	-0.59	1.00	0.20	0.79
2b	5.94	2.71	3.23	-0.77	1.14	0.21	0.98

4.4.8. Ionization potential, electron affinity and reorganization energy

IP and EA of organic molecules are important tools which provide relevant information about the charge transport property and charge injection character of a molecule.[81] Adiabatic IP and EA of these six molecules are calculated at B3LYP/6-311++G(d,p) functional and represented in Table 4.4. The IP and EA of studied dyes are in the range of 6.81 eV to 7.29 eV and 1.54 eV to 2.23 eV respectively. It is known that molecule with higher EA value shows higher electron transport ability and molecule with lower IP value shows higher hole transport ability. Compound **1a** has lowest IP value of 6.81 eV and **2c** has highest EA value of 2.23 eV. So **1a** and **2c** molecules will transport hole and electron better than the other molecules. It is interesting to note that with the decrease of HOMO-LUMO gap both in alkene and alkyne π-linker substituted systems IP values and EA values increase.

Table 4.4. Calculated ionization potentials (IP) , electron affinities (EA), reorganization energies (λ_{hole} and $\lambda_{electron}$), chemical potential ($\mu_{c.p}$), chemical hardness (η) and softess (s) of the dyes in gas phase at the B3LYP/6-311++G(d,p) level of theory.

Molecule	IP (eV)	EA (eV)	λ_{hole} (eV)	$\lambda_{electron}$ (eV)	$\mu_{c.p}$ (eV)	η (eV)	s (eV)
1a	6.81	1.54	0.37	0.35	4.23	1.45	0.68
1b	6.91	2.03	0.32	0.37	4.51	1.29	0.77
1c	7.06	2.17	0.28	0.30	4.65	1.25	0.8
2a	7.04	1.58	0.27	0.32	4.35	1.49	0.67
2b	7.11	2.05	0.26	0.35	4.48	1.46	0.68
2c	7.29	2.23	0.21	0.28	4.79	1.31	0.76

Reorganization energy of organic molecule gives idea about the rate of charge transport for DSSC application. Smaller the hole transport reorganization energy (λ_{hole}) better the hole transport material (HTM) and smaller the electron transport reorganization energy ($\lambda_{electron}$) better the electron transport material (ETM). Calculated values of λ_{hole}

and $\lambda_{electron}$ are given in Table 4.4 from which we find some significant results, such as with the increase in the strength of EWG, λ_{hole} values starts decreasing; substitution of alkene π-linker by alkyne π-linker, both hole and electron transport properties increases and in most of the cases except compound **1a** hole transport rate is higher than the electron transport rate. Also if we look on the alkene and alkyne π-linker series we find chemical hardness decreases whereas chemical potential and softness increase from weak EWG to strong EWG. Thus, the present results demonstrate that compound **2c** has lowest λ_{hole} and $\lambda_{electron}$ values of 0.214 eV and 0.28 eV respectively. This indicates that, compound **2c** can act as HTM as well as ETM. Compared to **1b** and **2b** dyes, **2b** shows low reorganization energy for both hole and electron than **1b** dye. So, dye **2b** should transport charge better for DSSC applications.

4.5. Conclusion

Extensive theoretical studies on the six newly designed molecules have been carried out in search of better NLO materials. We choose different D-π-A systems containing –CN and –COOH as electron acceptor group, indole as electron donor and thiazole ring with alkene or alkyne as π-conjugator. Our results show that all the studied dyes have narrow HOMO-LUMO gap in gas and solvent phases. Dye **2c** shows better planarity compare to other molecules. With increasing the strength of EWG at electron acceptor position, HOMO-LUMO gap decreases for both alkene and alkyne systems. From FMO analysis we find that donor unit stabilizes the HOMO, whereas acceptor unit stabilizes the LUMO. Thiazole ring also provides additional stabilization to the LUMO. In case of alkene substituted dyes the HOMO is more stabilized by π-bridge than thiazole ring and in case of alkyne substituted dyes reverse order is found. Photophysical properties of the six compounds are evaluated examining the excited states. TDDFT results show that all the dye exhibit λ_{max} in the visible region possessing low transition energy, high oscillator strength and LHE value. Maximum absorption wave length is found for **1c** which is well correlated with the HOMO-LUMO gap. All the investigated dyes show large NLO property. Among the studied dyes, **1c** has maximum $\Delta\alpha$ in gas and

in DMSO which is proportional to their dipole moments. It has been found that first and second-order hyperpolarizabilities are more favoured in alkyne substituted π-linker system. Compound **2c** shows highest β_{total} and γ_{total} value. Polarizability and hyperpolarizability increases with the solvent polarity. The computed β_{total} values are 326-587 times greater than the values of urea. Furthermore, hyperpolarizability increases with the increase of strength of EWG. Photo-voltaic property has been calculated for compound **1b** and **2b**. Substitution of alkene π-linker in **1b** by alkyne π-linker in **2b**, all relevant properties for DSSC application like electron injection free enthalpy, LHE, dipole moment, open circuit voltage, charge transport character are favoured. This improvement assists to obtain high J_{SC} as well as high power conversion efficiency. We also find that compound **2c** demonstrates lowest λ_{hole} and $\lambda_{electron}$ values. This indicates, compound **2c** can act both as HTM and ETM. If we look on the series we can see, chemical hardness decreases whereas chemical potential and softness increases from weak EWG to strong EWG. In all the cases alkyne systems prove better than the alkene systems for NLO and DSSC applications. Therefore, as a whole one can conclude that these six designed dyes can function as NLO material, among them compound **2c** shows highest NLO efficiency and **2b** demonstrates good photovoltaic property for DSSC application. This type of dye can be adsorbed on the surface of the titanium dioxide semiconductor and may be considered for future work. These results should be useful to design efficient NLO material and organic sensitizer in DSSC application.

4.6. References

1. Li, F.; Zheng, Q.; Yang, G.; Dai, N.; Lu, P., *Mater. Letters*, **2008**, *62*, 3059-3062;
2. Hu, X.; Jiang, P.; Ding, C.; Yang, H.; Gong, Q. *Nat. Photonics*, **2008**, *2*, 185;
3. Hagen, R.; Bieringer, T., *Adv. Mater*, **2001**, *13*, 1805-1810;
4. Beverina, L.; Fu, J.; Leclercq, A.; Zojer, E.; Pacher, P.; Barlow, S.; Van Stryland, E. W.; Hagan, D. J.; Brédas, J.-L.; Marder, S. R., *J. Am. Chem. Soc.*, **2005**, *127*, 7282-7283.
5. Teran, N. B.; He, G. S.; Baev, A.; Shi, Y.; Swihart, M. T.; Prasad, P. N.; Marks, T. J.; Reynolds, J. R., *J. Am. Chem. Soc.*, **2016**, *138*, 6975-6984;
6. Ishow, E.; Bellaïche, C.; Bouteiller, L.; Nakatani, K.; Delaire, J. A., *J. Am. Chem. Soc.*, **2003**, *125*, 15744-15745;
7. Hales, J. M.; Matichak, J.; Barlow, S.; Ohira, S.; Yesudas, K.; Brédas, J.-L.; Perry, J. W.; Marder, S. R., *Science*, **2010**, *327*, 1485-1488.

8. Liao, H.; Noguchi, M.; Maruyama, T.; Muragaki, Y.; Kobayashi, E.; Iseki, H.; Sakuma, I., *Med. Image Anal.*, **2012**, *16*, 754-766.
9. Tong, L.; Cheng, J.-X., *Mater. Today*, **2011**, *14*, 264-273.
10. Lupo, D., Wiley Online Library, **1995**. Molecular Nonlinear Optics: Materials, Physics, and Devices. Edited by J. Zyss, Academic Press, San Diego. CA 1994, XIII, 478 pp., hardcover, ISBN 0–12–784450–3
11. Park, K. H.; Lim, J. T.; Song, S.; Lee, Y. S.; Lee, C. J.; Kim, N., *Reac. Funct. Polym.*, **1999**, *40*, 177-184;
12. Wang, S.; Zhao, L.; Zhang, X.; Zhang, X.; Shi, Z.; Cui, Z.; Chen, X.; Yang, Y., *Polym. Int.*, **2009**, *58*, 933-938.
13. Zhou, X.-H.; Davies, J.; Huang, S.; Luo, J.; Shi, Z.; Polishak, B.; Cheng, Y.-J.; Kim, T.-D.; Johnson, L.; Jen, A., A. Jen, *J. Mater. Chem.*, **2011**, *21*, 4437-4444;
14. Kang, H.; Evmenenko, G.; Dutta, P.; Clays, K.; Song, K.; Marks, T. J., *J. Am. Chem. Soc.*, **2006**, *128*, 6194-6205.
15. Dalton, L. R.; Sullivan, P. A.; Bale, D. H., *Chem. Rev.*, **2009**, *110*, 25-55.
16. Andreu, R.; Blesa, M. J.; Carrasquer, L.; Garín, J.; Orduna, J.; Villacampa, B.; Alcalá, R.; Casado, J.; Ruiz Delgado, M. C.; López Navarrete, J. T., *J. Am. Chem. Soc.*, **2005**, *127*, 8835-8845.
17. Goswami,T; Misra, A., *J. Phys. Chem. A*, **2012**, *116*, 5207-5215.
18. Djebar, H.; Ali, R., *Med. J. Chem.*, **2015**, *4*, 185-192.
19. Yang, Y.; Liu, F.; Wang, H.; Bo, S.; Liu, J.; Qiu, L.; Zhen, Z.; Liu, X., *J. Mater. Chem. C*, **2015**, *3*, 5297-5306.
20. Raimundo, J.-M.; Blanchard, P.; Frere, P.; Mercier, N.; Ledoux-Rak, I.; Hierle, R.; Roncali, J., J. Roncali, *Tetrahedron Lett.*, **2001**, *42*, 1507-1510.
21. Zhang, Y.; Ortega, J.; Baumeister, U.; Folcia, C. s. L.; Sanz-Enguita, G.; Walker, C.; Rodriguez-Conde, S.; Etxebarria, J.; O'Callaghan, M. J.; More, K., *J. Am. Chem. Soc.*, **2012**, *134*, 16298-16306.
22. Luo, J.; Huang, S.; Cheng, Y.-J.; Kim, T.-D.; Shi, Z.; Zhou, X.-H.; Jen, A. K.-Y., *Org. Lett.*, **2007**, *9*, 4471-4474.
23. Rao, V. P.; Jen, A. K.; Wong, K.; Drost, K. J., *Tetrahedron Lett.*, **1993**, *34*, 1747-1750;
24. Cheng, L. T.; Tam, W.; Marder, S. R.; Stiegman, A. E.; Rikken, G.; Spangler, C. W., *J. Phys. Chem.*, **1991**, *95*, 10643-10652;
25. Miller, R. D.; Lee, V. Y.; Moylan, C. R., *Chem. Mater.*, **1994**, *6*, 1023-1032.
26. Gilchrist, T. L., *Heterocyclic Chemistry*, London : Pitman, New York, **1985**.
27. Nazim, M.; Ameen, S.; Akhtar, M. S.; Lee, Y.-S.; Shin, H.-S., *Chem. Phys. Lett.*, **2013**, *574*, 89-93
28. Melucci, M.; Favaretto, L.; Zanelli, A.; Cavallini, M.; Bongini, A.; Maccagnani, P.; Ostoja, P.; Derue, G.; Lazzaroni, R.; Barbarella, G., *Adv. Funct. Mater.*, **2010**, *20*, 445-452.
29. Moylan, C. R.; Twieg, R. J.; Lee, V. Y.; Swanson, S. A.; Betterton, K. M.; Miller, R. D., *J. Am. Chem. Soc.*, **1993**, *115*, 12599-12600;
30. Moylan, C. R.; Miller, R. D.; Twieg, R. J.; Betterton, K. M.; Lee, V. Y.; Matray, T. J.; Nguyen, C., *Chem. Mater.* **1993**, *5*, 1499-1508.
31. Calogero, G.; Di Marco, G.; Cazzanti, S., Caramori, S., Argazzi, R., Di Carlo, A.; Bignozzi, C. A., *Int. J. Mol. Sci.*, **2010**, *11*, 254-267.

32. Patil, D. S.; Avhad, K. C.; Sekar, N., *Comput. Theor. Chem.*, **2018**, *1138*, 75-83.
33. Nazim, M.; Ameen, S.; Akhtar, M. S.; Seo, H.-K.; Shin, H.-S., *RSC Adv.*, **2015**, *5*, 6286-6293.
34. Han, L.; Kang, R.; Zu, X.; Cui, Y.; Gao, J., *Photochem. Photobiol. Sci.* **2015**, *14*, 2046-2053.
35. Zhao, C.; Zhou, Y.; Lin, Q.; Zhu, L.; Feng, P.; Zhang, Y.; Cao, J., *J. Phys. Chem. B*, **2010**, *115*, 642-647.
36. Gong, W.; Li, Q.; Li, Z.; Lu, C.; Zhu, J.; Li, S.; Yang, J.; Cui, Y.; Qin, J., *J. Phys. Chem. B*, **2006**, *110*, 10241-10247;
37. Li, Q.; Li, Z.; Ye, C.; Qin, J., *J. Phys. Chem. B* **2008**, *112*, 4928-4933;
38. Li, Q.; Li, Z.; Zeng, F.; Gong, W.; Li, Z. a.; Zhu, Z.; Zeng, Q.; Yu, S.; Ye, C.; Qin, J., *J. Phys. Chem. B*, **2007**, *111*, 508-514.
39. Li, Q.; Lu, L.; Zhong, C.; Shi, J., Huang, Q., Jin, X., Peng, T.; Qin, J.; Li, Z., *J. Phys. Chem. B*, **2009**, *113*, 14588-14595;
40. Zhang, X.-H.; Cui, Y.; Katoh, R.; Koumura, N.; Hara, K., *J. Phys. Chem. C*, **2010**, *114*, 18283-18290;
41. Ruangsupapichat, N.; Ruamyart, M.; Kanchanarugee, P.; Boonthum, C., Prachumrak, N.; Sudyoadsuk, T.; Promarak, V. *Dyes Pigm.*, **2018**, *151*, 149-156;
42. Bisht, R.; Sudhakar, V.; Mele Kavungathodi, M. F.; Karjule, N.; Nithyanandhan, J., *ACS Appl. Mater. Interfaces*, **2018**, *10*, 26335-26347.
43. Chen, W.-C.; Nachimuthu, S.; Jiang, J.-C., *Sci. Rep.*, **2017**, *7*, 4979.
44. Badiger, J.; Manjulatha, K.; Girish, M.; Sharif, A.; Purohit, M. *ARKIVOC: Online J. Org. Chem.*, **2009**;
45. Jiang, X.; Tiwari, A.; Thompson, M., Chen, Z.; Cleary, T. P.; Lee, T. B., *Org. Process Res. Dev.*, **2001**, *5*, 604-608.
46. Achelle, S.; Barsella, A.; Caro, B.; Robin-le Guen, F., *RSC Adv.* **2015**, *5*, 39218-39227;
47. Tarsang, R.; Promarak, V.; Sudyoadsuk, T.; Namuangruk, S.; Kungwan, N.; Khongpracha, P.; Jungsuttiwong, S., *RSC Adv.*, **2015**, *5*, 38130-38140.
48. Karakas, A.; Elmali, A.; Unver, H., *Spectrochim. Acta A: Mol. Biomol. Spectrosc.*, **2007**, *68*, 567-572.
49. Chemate, S.; Sekar, N., *J. Fluoresc.*, **2016**, *26*, 2063-2077.
50. Curioni, A.; Boero, M.; Andreoni, W., *Chem. Phys. Lett.*, **1998**, *294*, 263-271.
51. Hutchison, G. R.; Ratner, M. A.; Marks, T. J., *J. Am. Chem. Soc.*, **2005**, *127*, 2339-2350.
52. Narayan, M. R., *Renew. Sust. Energ. Rev.*, **2012**, *16*, 208-215.
53. Zhang, J.; Li, H.-B.; Sun, S.-L.; Geng, Y.; Wu, Y.; Su, Z.-M., *J. Mater. Chem.*, **2012**, *22*, 568-576.
54. Sang-aroon, W.; Saekow, S.; Amornkitbamrung, V., *J. Photochem. Photobiol. A: Chem.*, **2012**, *236*, 35-40.
55. Katoh, R.; Furube, A.; Yoshihara, T.; Hara, K.; Fujihashi, G.; Takano, S.; Murata, S.; Arakawa, H.; Tachiya, M., *J. Phys. Chem. B*, **2004**, *108*, 4818-4822.
56. Ning, Z.; Fu, Y.; Tian, H., *Energ. Environment. Sci.* **2010**, *3*, 1170-1181.
57. Li, Y.; Pullerits, T.; Zhao, M.; Sun, M., *J. Phys. Chem. C* **2011**, *115*, 21865-21873;
58. Scholes, G. D.; Rumbles, G., *Nat. Mater.*, **2006**, *5*, 683.

59. Frisch, M. J.; Trucks, G. W.; Schlegel, H. B.; Scuseria, G. E.; Robb, M. A.; Cheeseman, J. R.; Scalmani, G.; Barone, V.; Mennucci, B.; Petersson, G. A. et al. Gaussian 09, Revision B.01. In Wallingford CT, 2009.
60. Thakare, S. S.; Chakraborty, G.; Krishnakumar, P.; Ray, A. K.; Maity, D. K.; Pal, H.; Sekar, N., *J. Phys. Chem. B*, **2016,** 120, (43), 11266-11278.
61. Cossi, M.; Barone, V., *J. Chem. Phys.*, **2001,** 115, (10), 4708-4717.
62. Barone, V.; Cossi, M., *J. Phys. Chem. A*, **1998,** 102, (11), 1995-2001.
63. Yanai, T.; Tew, D. P.; Handy, N. C., *Chem. Phys. Lett.* **2004,** 393, (1-3), 51-57.
64. Lu, T., Multiwfn. *Software manual. Version* **2014,** 3, (6).
65. Kutzelnigg, W., Atoms in Molecules. A Quantum Theory.(Reihe: International Series of Monographs on Chemistry, Vol. 22.) Von RFW Bader. Clarendon Press, Oxford, 1990. XVIII, 438 S., geb.£ 50.00.–ISBN 0-19-855168-1. *Angewandte Chemie* **1992,** 104, (10), 1423-1423.
66. Solomon, R. V.; Veerapandian, P.; Vedha, S. A.; Venuvanalingam, P., *J. Phys. Chem. A*, **2012,** 116, (18), 4667-4677.
67. Wen, Y.; Yang, H.; Zheng, D.; Sun, K.; Wang, L.; Zhang, J., *J. Phys. Chem. C*, **2017,** 121, (26), 14019-14026.
68. Zhang, W.; Wu, J.; Wen, Y.; Wu, W.; Wang, L., *Dyes Pigm.*, **2018,** 149, 908-914.
69. Gunasekaran, S.; Balaji, R. A.; Kumeresan, S.; Anand, G.; Srinivasan, S., *Can. J. Anal. Sci. Spectrosc.*, **2008,** 53, 149-160.
70. Steckler, T. T.; Henriksson, P.; Mollinger, S.; Lundin, A.; Salleo, A.; Andersson, M. R., *J. Am. Chem. Soc.*, **2014,** 136, (4), 1190-1193.
71. Chattaraj, P. K.; Roy, D. R., *Chem. Rev.*, **2007,** 107, (9), PR46-PR74.
72. He, Q.; Li, Q.; Khene, S.; Ren, X.; López-Suárez, F. E.; Lozano-Castelló, D.; Bueno-López, A.; Wu, G., *J. Phys. Chem. C*, **2013,** 117, (17), 8697-8707.
73. Grätzel, M., *Nature*, **2001,** 414, (6861), 338.
74. Kim, B. G.; Chung, K.; Kim, J., *Chem.-A Eur. J.*, **2013,** 19, (17), 5220-5230.
75. Wu, Y.; Zhu, W., *Chem. Soc. Rev.*, **2013,** 42, (5), 2039-2058.
76. Ozawa, H.; Okuyama, Y.; Arakawa, H., *ChemPhysChem*, **2014,** 15, (6), 1201-1206.
77. Prakasam, M.; Anbarasan, P., *RSC Adv.*, **2016,** 6, (79), 75242-75250.
78. Mendis, B. S.; de Silva, K. N., *J. Mol. Str.: THEOCHEM*, **2004,** 678, (1-3), 31-38.
79. Cheng, L. T.; Tam, W.; Stevenson, S. H.; Meredith, G. R.; Rikken, G.; Marder, S. R., *J. Phys. Chem.*, **1991,** 95, (26), 10631-10643.
80. Yu. Balakina, M.; Nefediev, S. E., *Int. J. Quant. Chem.*, **2006,** 106, (10), 2245-2253.
81. Happ, B.; Winter, A.; Hager, M. D.; Schubert, U. S., *Chem. Soc. Rev.*, **2012,** 41, (6), 2222-2255.